Low-Latency Searches for Gravitational Waves Using the GstLAL Data Analysis Pipeline

Amanda C. Baylor
Department of Physics, University of Wisconsin-Milwaukee
Milwaukee, WI, USA

Abstract

Compact binary mergers involving at least one neutron star could produce electromagnetic counterparts. Prompt alerts of the detection of gravitational waves (GWs) from these mergers allow for rapid follow-up on the sources and the potential detection of new physics surrounding their astrophysical processes. The GstLAL pipeline searches for and analyzes GW signals in low-latency, producing results in near real time. For more efficient EM follow-up, we focus on the development of early warning (EW) detections, which are alerts sent out prior to merger. We perform tests of an EW GstLAL pipeline using simulated signals in preparation for the LIGO-Virgo-KAGRA collaboration's fourth observing run (O4). We also discuss the prospects for sending out an EW alert and localizing the signal with a four detector network.

1. Introduction

Following the first detection of gravitational waves (GWs) from a binary neutron star (BNS) merger, GW170817, by the LIGO Scientific Collaboration in 2017 (Abbott et al. 2017b), we have unlocked a new era of multi-messenger astronomy. Gamma-ray burst GRB 170817A was jointly observed by the Fermi Gamma-ray Burst Monitor approximately 1.7 seconds after the merger (Abbott et al. 2017a). Electromagnetic (EM) follow-up was also performed by UV, optical, infra-red, and radio telescopes (Abbott et al. 2017c). Events with EM counterparts could improve our understanding of high-energy astrophysical events, provide us with new measurements of cosmological parameters, and help us study the fundamental physics of gravity.

The strongest GW signals are generated by compact binary coalescences (CBCs), such as binary black hole (BBH), BNS, and neutron star-black hole (NSBH) mergers. EM counterparts can be produced by mergers involving at least one neutron star, and it is crucial that we provide timely alerts to partner EM facilities for prompt follow-up. The GstLAL data analysis pipeline searches for and detects GW signals from CBCs using matched-filtering (Sec. 2.1). GstLAL operates in low-latency, meaning that there is minimal delay between data acquisition and alert generation. The LIGO-Virgo-KAGRA (LVK) collaboration is expected to begin the fourth observing run (O4) with a network of four GW interferometers in May 2023. The detectors are improving their range sensitivity by a factor of ~ 1.5, which translates to an increase of $1.5^3 \sim 3$ times the number of detections. This will allow for better localization of sources and greater opportunity for GstLAL to identify events with EM counterparts.

In this work, we focus on the development of the early warning (EW) framework for GstLAL (Sachdev et al. 2020; Magee et al. 2021). The goal of EW is such that alerts are sent to partner EM facilities *before* the objects collide and merge. This would allow us to capture vital information about the physics at the point of merger. We elaborate on the methods used by GstLAL to search for GW signals and identify candidate events in Sec. 2. In Sec. 3 we review the results of tests of the EW configuration and conclude with a discussion in Sec. 4.

2. Methods

GstLAL uses matched-filtering to identify GW candidates. Once the pipeline identifies a candidate event, it assigns a ranking statistic based on candidate properties and instrument sensitivity to estimate significance.

2.1. Matched-filtering Matched-filtering is a method to extract signals from noisy data by cross-correlating the detector output with a template gravitational waveform signal (Allen et al. 2012). The shape of the waveform is predicted by general relativity and depends on the parameters of the source. Some parameters are intrinsic to the

binary, such as masses and spins. Extrinsic parameters are those related to the position of the source with respect to the observer, including distance and inclination angle. In order to account for a variety of binary systems with different parameters, we create a template bank containing a discrete set of waveforms that spans the intrinsic parameter space of the search. The goal is to maximize the matched-filter output for the intrinsic parameters using the template bank. Maximization of the extrinsic parameters is done analytically.

To make the template bank more efficient for matched-filtering, the Low Latency Online Inspiral Detection (LLOID) method is used (Cannon et al. 2012). This method uses singular value decomposition (SVD) to produce a set of orthonormal filters that is more computationally efficient to use than the original bank. The templates are binned by effective spin

$$\chi_{\text{eff}} \equiv \frac{m_1\chi_1 + m_2\chi_2}{m_1 + m_2} \tag{1}$$

and chirp mass

$$\mathcal{M} = \frac{(m_1 m_2)^{3/5}}{(m_1 + m_2)^{1/5}} \tag{2}$$

where m_1, m_2 are the component masses and χ_1, χ_2 are the dimensionless component spins aligned with the orbital angular momentum. Prior to LLOID decomposition, the template bank is split into 'split-banks' of templates that have similar parameters. In order to mitigate boundary effects from SVD, we overlap templates between adjacent split-banks. We then perform matched-filtering using this reduced set of filters.

The output of matched-filtering is a signal-to-noise ratio (SNR), which is how loud the signal is compared to the noise present. GstLAL calculates SNR in the time-domain (Messick et al. 2017),

$$x_i(t) = 2\int_{-\infty}^{\infty} df \frac{\tilde{h}_i^*(f)\tilde{d}(f)}{S_n(|f|)} e^{2\pi i f t} \tag{3}$$

which is the inner product of the data d with the template h. $x_i(t)$ is the real-valued SNR using the ith template, f denotes frequency, and $S_n(f)$ is the single-sided noise PSD. Data from each detector contains non-astrophysical noise transients called glitches, which cause GstLAL to record high peaks in the SNR time series, so SNR alone is not enough to distinguish noise from actual signals. Therefore, the pipeline performs signal consistency tests (Sachdev et al. 2019) to determine the validity of a peak.

If the SNR passes a preset threshold, GstLAL produces a trigger. Triggers are defined by the recorded SNR, the results of the signal consistency test, the masses and spins of the template used, and the phase and time of coalescence. Triggers found to be coincident in multiple detectors are elevated to the status of an event, while triggers that are not coincident are considered to be just noise.

BNS systems have long inspirals and will spend approximately 10-15 minutes in the band of the GW detectors at design sensitivity (Sachdev et al. 2020). Unlike BBH signals, which are much shorter in duration, BNS signals are ideal for EW detection. In principle, GstLAL can use matched-filtering to accumulate enough SNR to identify a forthcoming event and produce an alert up to about a minute prior to merger. We test the performance of matched-filtering using our bank of template waveforms described in Sec. 3, which we have constructed for an EW configuration.

2.2. Ranking Statistics We discard candidates with an SNR below 4 to reduce the volume of triggers, but those that survive are then assigned a likelihood ratio (LR) (Cannon et al. 2015; Sachdev et al. 2019, 2020; Hanna et al. 2020; Messick et al. 2017). Since detector noise is non-Gaussian and not stationary, SNR is not an optimal detection

statistic, and we instead use the LR to rank candidates from least likely to most likely to be a signal. The LR is defined as the ratio of probability of certain observables given the signal hypothesis versus the noise hypothesis (Hanna et al. 2020),

$$\mathcal{L} = \frac{P(\vec{D_H}, \vec{O}, \vec{\rho}, \vec{\xi^2}, \vec{\phi}, \vec{t} \mid signal)}{P(\vec{D_H}, \vec{O}, \vec{\rho}, \vec{\xi^2}, \vec{\phi}, \vec{t} \mid noise)} \tag{4}$$

where $\vec{D_H}$ is a vector of horizon distances for each observatory, $\vec{O}$ is the set of detectors that observed the event in coincidence, $\vec{\rho}$ is a vector of SNRs in each detector, $\vec{\xi^2}$ is a vector representing the signal consistency test in each detector, and $\vec{\phi}$ and $\vec{t}$ are the phases and times measured in each detector. Components of the LR are dependent on the sensitivity of the instrument at the time of detection.

The false alarm rate (FAR), or number of false alarms per unit time, is calculated using the logarithm of the LR (Messick et al. 2017),

$$\text{FAR} = \frac{C(\ln\mathcal{L}^* \mid noise)}{T} \tag{5}$$

where $\mathcal{L}^*$ is the LR threshold, T is the experiment length, and $C(\ln\mathcal{L}^* \mid noise)$ is the complementary cumulative distribution,

$$C(\ln\mathcal{L}^* \mid noise) = \int_{\ln\mathcal{L}^*}^{\infty} \mathrm{d}\ \ln\mathcal{L}\ P(\ln\mathcal{L} \mid noise). \tag{6}$$

Eq. 5 describes how often a candidate with $\ln\mathcal{L} \geq \ln\mathcal{L}^*$ is expected to be produced from noise. For example, a FAR of 1/(30 days) means that we would expect noise to produce a LR as high as the event's once every 30 days. FAR is used to rank events by their significance, with a lower FAR characterizing a more significant event. In the current GstLAL framework, candidate events that pass a given FAR threshold are identified within $\sim$ 12 seconds of the GW signal arriving at Earth, with $\sim$ 25 seconds of total alert latency (Magee et al. 2021).

3. Results

The pipeline can operate in two different modes: *offline* and *online*. In offline mode, we perform analyses with the full data set. Offline mode is used to tune the pipeline and obtain more refined information about the data quality. In online mode, we replay the data collection to simulate real-time data analysis. This allows us to test the pipeline's ability to send out alerts prior to merger.

We present the results of offline runs using GstLAL in an EW configuration. Our goal is to maximize the sensitivity of the search. We generate one month of stationary Gaussian data recolored to Advanced LIGO and Advanced Virgo design sensitivities and inject simulated BNS signals in order to compute the sensitivity of our search. We construct a template bank consisting of non-spinning BNS waveforms with masses $(1 - 2.4)\mathrm{M}_{\odot}$. Finally, we run the pipeline end-to-end to study how well our template bank performs in recovering injections with their expected parameters.

We begin matched-filtering at 10 Hz but conclude filtering at various max final frequencies, with each one corresponding to various times before merger. The search is conducted for 29 Hz, 32 Hz, 38 Hz, 49 Hz, 56 Hz, and 1024 Hz cut-off frequencies to analyze injection recovery at $\sim$ 58 s, 44 s, 28 s, 14 s, 10 s, and 0 s before merger respectively. We consider our injections 'found' if, at the time of injection, a coincident event is found with the correct template parameters and a FAR $\leq$ 1/(30 days) (FAR $\lesssim 10^{-7}$ Hz) and 'missed' otherwise.

For each of the six offline runs, we first consider the 'closed box' results. In a closed box analysis, we blind ourselves

to real signals to make sure the pipeline is working correctly. Thus, we expect that the pipeline is recovering only noise. We look at the recovered signals after 'opening' the box.

The closed box result is prepared by looking at time-shifted coincidences between two or more detectors. The pipeline only treats coincident events as candidates, so non-coincident triggers should closely follow the background model. Fig. 1 shows the money plots of two separate 29 Hz runs with different configurations. Our initial configuration consisted of an overlap of 30 and 2 split-banks, while our 'tuned' run has an overlap of 50 and 5 split-banks. Recall that the overlap is the number of overlapping templates between adjacent split-banks. The number of split-banks here indicates how many split-banks are grouped together in one SVD bin.

The plots of Fig. 1 demonstrate that, in the absence of real GW signals, the distribution is consistent with noise. The bottom plot, or the tuned version, follows the noise distribution more closely, so we proceed with this configuration for our future analyses. The closer we follow the noise distribution, the more confident we are that the pipeline is not making any false detections. Recall that a lower FAR (higher inverse FAR) is desirable for a real detection, which would fall outside of the noise distribution on a money plot.

Another useful result to consider from our offline runs is the search sensitivity range. Fig. 2 shows the sensitivity ranges for the 29 Hz run and the 56 Hz run. The ranges indicate the distance at which we are sensitive to for detecting these BNS signals based on their FAR threshold. We see that we are sensitive to farther ranges at a higher frequency cut-off, but at the cost of having less time before merger to provide an EW alert. These plots help us to choose a configuration that is best for the desired search.

4. Discussion

Once GstLAL identifies an event, rapid sky localization is executed by BAYESTAR (Singer & Price 2016), a fast Bayesian algorithm that can reconstruct positions of GW transients using the output provided by matched-filtering. GstLAL uses matched-filtering to generate the SNR time series of all signals that pass the FAR threshold and then provides these to BAYESTAR. In the low-latency framework, BAYESTAR can estimate the event's sky position within seconds (Magee et al. 2021). Since the earliest we could provide an EW alert would be 60 s before merger, we need fast and accurate sky localization. BAYESTAR was optimized to support EW localizations, taking about 0.5 s per event for EW triggers and 1.1 s per event for non-EW triggers (Magee et al. 2021). Sky localization improves the closer to merger the binary is, but we are able to provide estimates earlier. Well-localized CBCs which we are able to provide EW alerts for will be those that are closer to us, enabling for better EM follow-up.

GstLAL is able to identify candidate events in low-latency with their significance and provide point estimates for binary parameters. More thorough parameter estimation is performed later (Veitch et al. 2015; Ashton et al. 2019; Rose et al. 2022) on a timescale of hours to days after detection. In order to test the pipeline's sensitivity to different regions of the binary parameter space, different sets of injections must be used in our offline runs. Here we demonstrate results for a BNS template bank, but we plan to expand our bank to include NSBH waveforms. We will also execute searches in online mode to simulate real-time data analysis in preparation for O4. With our offline runs, we have so far been able to tune the pipeline and determine optimal configurations for our desired searches.

The LVK's third observing run (O3) had a detection range for BNS mergers of up to 133 Mpc (Abbott et al. 2021). The projected sensitivity range for O4 is up to 190 Mpc. Given the detection rates in O3, the LVK expects to make ~ 10 BNS and ~ 5 NSBH detections in O4. We have demonstrated here that with this configuration, GstLAL is capable of identifying BNS systems out to 100 Mpc approximately 60 s before merger and out to 210 Mpc approximately 10 s before merger at the desired FAR threshold of $\sim 10^{-7}$ Hz. Thus, this work aids in the possibility of making an EW detection in O4.

With zero latency, we expect ~ 2 BNS events to be observable 60 s before coalescence with a network of 4 detectors (Magee et al. 2021). There is an increase in latency due to the time needed to process and transfer the data after acquisition at the detectors, which is ~ 12 s (Messick et al. 2017). Current efforts are focused on reducing this latency prior to O4.

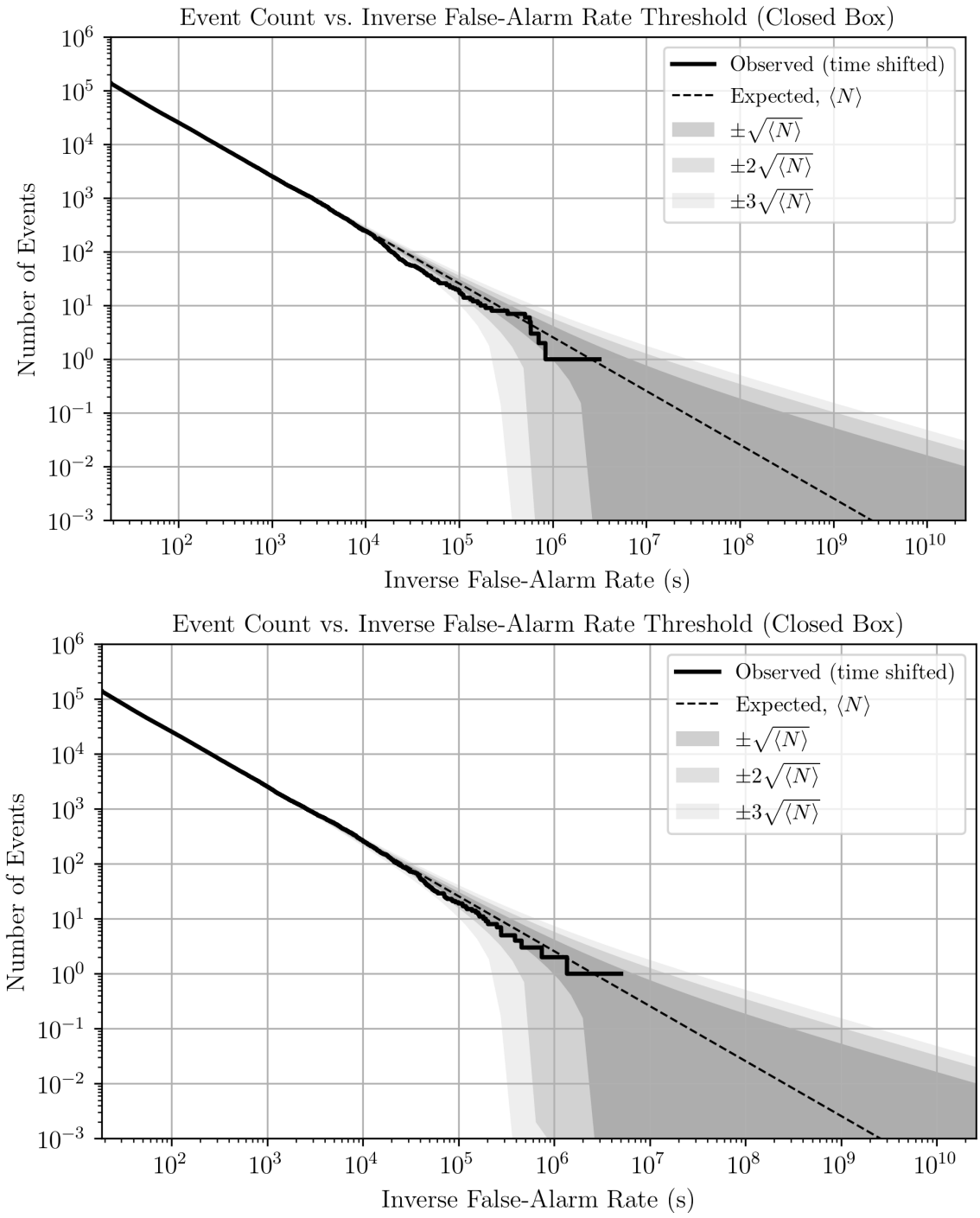

Figure 1: Money plots for two separate offline 29 Hz runs. The top plot represents the initial configuration with an overlap of 30 and 2 split-banks. The bottom plot is a tuned version with an overlap of 50 and 5 split-banks. The black line is the observed number of events, or the triggers that passed the SNR threshold, and the shaded regions are the noise distributions $\langle N \rangle$. Since the plot is truncated before we make the first real detection at the inverse FAR threshold of $\sim 10^7$ s, we expect the black line to always fall within the noise. We see that the tuned version follows the noise distribution more closely.

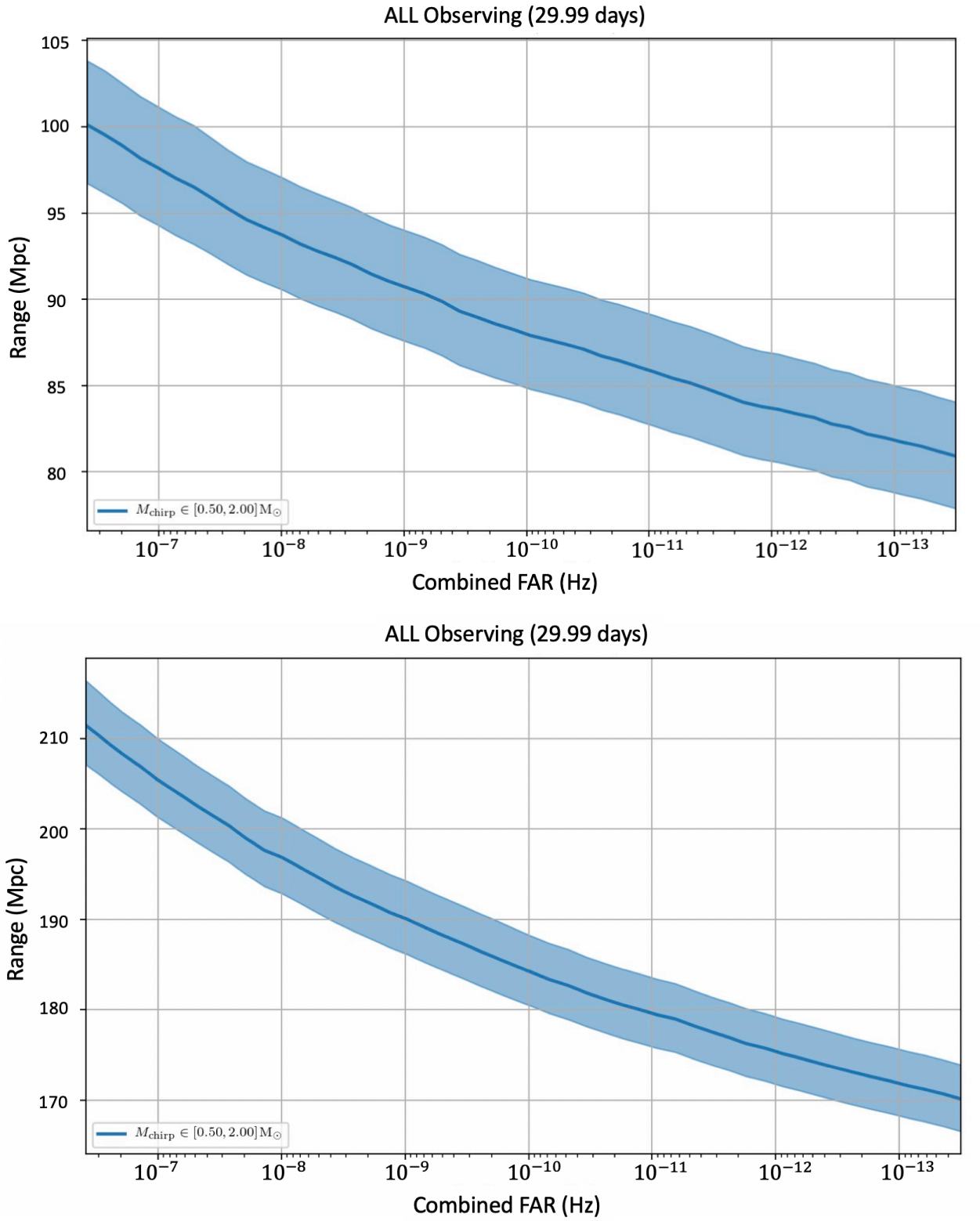

Figure 2: Range sensitivity plots for the 29 Hz (top) and 56 Hz (bottom) offline runs using one month of stationary Gaussian data recolored to Advanced LIGO and Advanced Virgo design sensitivities injected with simulated BNS signals. The threshold for found injections is FAR $\lesssim 10^{-7}$ Hz. The pipeline is sensitive to BNS signals at these distances (in Mpc) with these FARs for chirp masses between $(0.5 - 2.0)\text{M}_\odot$.

5. Acknowledgments

We thank Surabhi Sachdev and Pratyusava Baral for useful comments and discussion which improved this work. This work makes use of the `gstlal` (`https://lscsoft.docs.ligo.org/gstlal/`) software package. The author is grateful for resources provided by the LVK collaboration and supported by National Science Foundation Grant PHY-2207728, and those provided by the Leonard E. Parker Center for Gravitation, Cosmology and Astrophysics at the University of Wisconsin-Milwaukee. This material is based upon work supported by NASA under Award No. RFP22_3-0 issued through the Wisconsin Space Grant Consortium and the National Space Grant College and Fellowship Program, and any opinions, findings, and conclusions or recommendations expressed in this material are those of the authors and do not necessarily reflect the views of the National Aeronautics and Space Administration.

References

Abbott, BP; et al. "Gravitational waves and gamma-rays from a binary neutron star merger: Gw170817 and grb 170817a," *The Astrophysical Journal Letters*, v. 848(2), 2017a, p. L13

Abbott, BP; et al. "GW170817: Observation of gravitational waves from a binary neutron star inspiral," *Physical Review Letters*, v. 119(16), 2017b

Abbott, BP; et al. "Multi-messenger observations of a binary neutron star merger," *The Astrophysical Journal*, v. 848(2), 2017c, p. L12

Abbott, R; et al. "GWTC-3: Compact binary coalescences observed by ligo and virgo during the second part of the third observing run", 2021

Allen, B; Anderson, WG; Brady, PR; Brown, DA; Creighton, JDE. "Findchirp: An algorithm for detection of gravitational waves from inspiraling compact binaries," *Phys. Rev. D*, v. 85, 2012, p. 122006

Ashton, G; Hübner, M; Lasky, PD; Talbot, C; Ackley, K; Biscoveanu, S; Chu, Q; Divakarla, A; Easter, PJ; Goncharov, B; Vivanco, FH; Harms, J; Lower, ME; Meadors, GD; Melchor, D; Payne, E; Pitkin, MD; Powell, J; Sarin, N; Smith, RJE; Thrane, E. "Bilby: A user-friendly bayesian inference library for gravitational-wave astronomy," *The Astrophysical Journal Supplement Series*, v. 241(2), 2019, p. 27

Cannon, K; Cariou, R; Chapman, A; Crispin-Ortuzar, M; Fotopoulos, N; Frei, M; Hanna, C; Kara, E; Keppel, D; Liao, L; Privitera, S; Searle, A; Singer, L; Weinstein, A. "Toward Early-warning Detection of Gravitational Waves from Compact Binary Coalescence," *ApJ*, v. 748(2), 2012, p. 136. https://ui.adsabs.harvard.edu/abs/2012ApJ...748..136C

Cannon, K; Hanna, C; Peoples, J. "Likelihood-ratio ranking statistic for compact binary coalescence candidates with rate estimation", 2015

Hanna, C; Caudill, S; Messick, C; et al. "Fast evaluation of multidetector consistency for real-time gravitational wave searches," *Physical Review D*, v. 101(2), 2020

Magee, R; Chatterjee, D; Singer, LP; et al. "First demonstration of early warning gravitational-wave alerts," *The Astrophysical Journal Letters*, v. 910(2), 2021, p. L21

Messick, C; Blackburn, K; Brady, P; et al. "Analysis framework for the prompt discovery of compact binary mergers in gravitational-wave data," *Physical Review D*, v. 95(4), 2017

Rose, CA; Valsan, V; Brady, PR; Walsh, S; Pankow, C. "Supplementing rapid bayesian parameter estimation schemes with adaptive grids", 2022

Sachdev, S; Caudill, S; Fong, H; et al. "The gstlal search analysis methods for compact binary mergers in advanced ligo's second and advanced virgo's first observing runs," *arXiv: General Relativity and Quantum Cosmology*, 2019

Sachdev, S; Magee, R; Hanna, C; et al. "An early-warning system for electromagnetic follow-up of gravitational-wave events," *The Astrophysical Journal Letters*, v. 905(2), 2020, p. L25

Singer, LP; Price, LR. “Rapid bayesian position reconstruction for gravitational-wave transients,” *Physical Review D*, v. 93(2), 2016

Veitch, J; Raymond, V; Farr, B; Farr, W; Graff, P; Vitale, S; Aylott, B; Blackburn, K; Christensen, N; Coughlin, M; Pozzo, WD; Feroz, F; Gair, J; Haster, CJ; Kalogera, V; Littenberg, T; Mandel, I; O’Shaughnessy, R; Pitkin, M; Rodriguez, C; Röver, C; Sidery, T; Smith, R; Sluys, MVD; Vecchio, A; Vousden, W; Wade, L. “Parameter estimation for compact binaries with ground-based gravitational-wave observations using the LALInference software library,” *Physical Review D*, v. 91(4), 2015